J. Comp. Path. 2018, Vol. 159, 11–15

Available online at www.sciencedirect.com

ScienceDirect

ELSEVIER

www.elsevier.com/locate/jcpa

NEOPLASTIC DISEASE

Pulmonary Basaloid Squamous Cell Carcinoma in a Dog

A. Morey-Matamalas*, A. de Stefani†, D. Corbetta‡, L. Grau-Roma‡ and S. de Brot‡

* *Institute for Research in Biomedicine, Baldiri Reixac 10, Barcelona, Spain,* † *Dick White Referrals, Six Mile Bottom and* ‡ *School of Veterinary Medicine and Science, University of Nottingham, Sutton Bonington, UK*

Summary

A 9-year-old neutered male crossbred dog with a 4-week history of progressive vestibulocerebellar signs was presented for necropsy examination. Gross examination revealed neoplastic growth in the lungs, thoracic lymph nodes, left kidney and cerebellum. Microscopically, the tumour consisted of an infiltrative, densely cellular, basaloid epithelial neoplastic growth with extensive areas of abrupt keratinization. Immunohistochemically, neoplastic cells expressed p63 and partially expressed cytokeratins 5/6. Based on these findings, the tumour was diagnosed as a primary pulmonary basaloid squamous cell carcinoma (BSSC) with metastasis to regional lymph nodes, kidney and brain. As far as the authors are aware, this is the first description of BSCC in an animal species.

Keywords: basaloid; dog; lung; squamous cell carcinoma

Lung neoplasia is uncommon in domestic animals, apart from in dogs and cats. The incidence of canine lung neoplasia increases with age and the most common primary tumour is bronchioalveolar carcinoma. Adenocarcinomas, adenosquamous and squamous cell carcinomas (SCCs) are less common (Meuten, 2017).

Basaloid squamous cell carcinoma (BSCC) is a rare neoplasm of the lung, which was first described in man in 1992 (Brambilla *et al.*, 1992). In the current 2015 World Health Organization (WHO) tumour classification, BSCC is considered to be a subtype of SCC (Travis *et al.*, 2015). Squamous markers, such as p40 and p63, are expressed consistently in BSCC (Bishop *et al.*, 2012; Travis *et al.*, 2015). Other lung tumour subtypes of SCC include keratinizing squamous cell carcinoma, non-keratinizing squamous cell carcinoma and squamous cell carcinoma *in situ* (Travis *et al.*, 2015). Comprehensive descriptions of pulmonary BSCC appear to be lacking in animals. One case report describes a poorly differentiated, not further classified, pulmonary SCC in a dolphin with histological features potentially compatible with BSCC (Ewing and Mignucci-Giannoni, 2003).

A 9-year-old neutered male crossbred dog was submitted for post-mortem examination. The animal was presented 3 days before for neurological examination with a 4-week history of progressive vestibulocerebellar signs. Serum biochemistry revealed elevated alkaline phosphatase (412.0 U/l, reference interval <130.0 U/l), total bilirubin (8.6 μmol/l, reference interval 0.1–4.2 μmol/l) and creatine kinase (334.0 U/l, reference interval 20.0–225.0 U/l) and a low sodium:potassium ratio (27.4, reference interval 28.8–40.0). Neurological examination localized a lesion within the caudal cranial fossa affecting the vestibulocerebellar structures. A degree of left lateralization of the lesion was considered possible based on the observed proprioceptive deficits. At this point, the main differential diagnoses included neoplasia or

Correspondence to: S. de Brot (e-mail: simone.debrot@nottingham.ac.uk).

0021-9975/$ - see front matter
https://doi.org/10.1016/j.jcpa.2017.12.007

inflammatory disease. A magnetic resonance imaging (MRI) examination of the brain revealed a rim-enhancing cerebellar mass measuring 1.1 × 1.3 cm located in the centre of the cerebellum, with associated perilesional oedema. Mild central compression of the brainstem and mild rostral transtentorial herniation with extension to the foramen magnum was observed. Cerebrospinal fluid (CSF) analysis revealed moderate to severe 'albuminocytological dissociation' (protein 2.40 g/l, reference interval 0.14–0.30 g/l; nucleated cell count 3.0×10^9/l, reference interval $0–6 \times 10^9$/l).

Given the clinical findings, the presence of a neoplastic lesion was considered highly likely, although an inflammatory lesion could not be excluded based on the diagnostic tests performed. Medical management with glucocorticoids and possible chemotherapy was proposed to the owners. However, the owners elected for humane destruction based on the poor prognosis and quality of life and gave consent for a full post-mortem examination.

On gross examination, the main lesions were observed in the lung, the left kidney and the cerebellum. The lung contained multifocal, variably sized, 0.3–4.0 cm diameter, raised spherical nodules that were pale tan in colour, often umbilicated, poorly demarcated, solid and with a firm, often gritty consistency. The two largest masses measured up to 3.5 × 3.0 × 4.0 cm and were located at the level of the bifurcation of the main bronchi and within the mediastinal edge of the left caudal lobe (Fig. 1). The remaining lung tissue was diffusely dark red, wet and heavy, compatible with congestion and oedema. Mediastinal, tracheobronchial and bronchial lymph nodes were enlarged (up to 1 × 1.5 cm) and expanded by similar tissue as described in the lungs, compatible with tumour metastasis. The left kidney contained a focal wedge-shaped, 0.6 × 0.8 × 0.5 cm, pale tan, solid mass within the cortex, compatible with tumour metastasis. On coronal serial sections of the brain, at the level of cerebellum and brainstem, a focal, irregularly-shaped, poorly demarcated, infiltrative, non-encapsulated, pale tan and firm mass was located centrally in the white matter of the cerebellum between the fourth ventricle and the cerebellar vermis (Fig. 2). Samples of all the main organs and lesions were fixed in 10% neutral buffered formalin, processed routinely and embedded in paraffin wax.

Microscopically, the lung nodules corresponded to non-encapsulated, infiltrative, densely cellular epithelial proliferations with extensive areas of abrupt keratinization (Fig. 3). The cells were mostly closely packed in a lobular or cribriform pattern, appeared basaloid and were supported by dense fibrous stroma. Proliferating, interpreted as neoplastic, cells often lined extensive lakes of keratin, and were round to polygonal with round, hyperchromatic nuclei and mostly scant cytoplasm. Nuclear palisading was frequent, compatible with a basaloid cellular differentiation. Distinct intercellular bridges were not observed. Mitotic activity was moderate (0–6 mitoses per ×400 high-power field). Within the cellular mass there were multifocal extensive areas of necrosis, some admixed with abundant neutrophils and often with foci of dystrophic calcification. Multifocal intrapulmonary micrometastases were present.

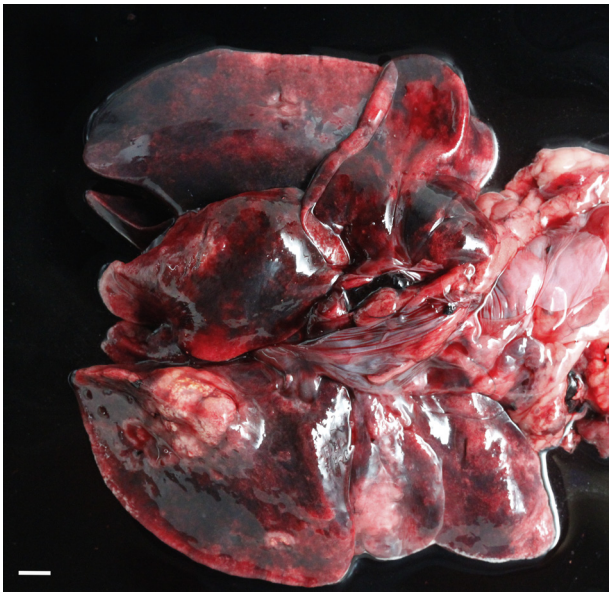

Fig. 1. Lung with BSCC, ventral view. Note the multiple, poorly demarcated, pale tan, slightly raised neoplastic nodules in the lung parenchyma. Remaining lung tissue is markedly congested and oedematous. Bar, 1 cm.

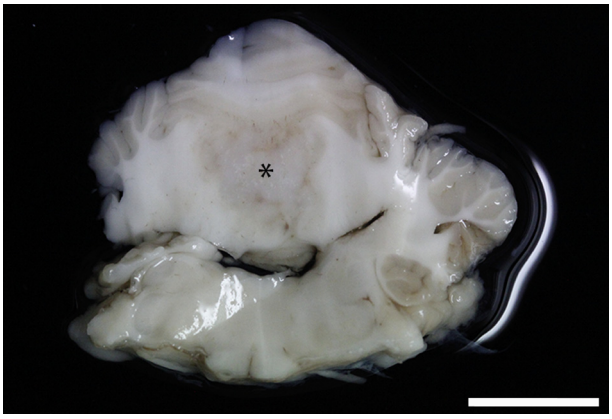

Fig. 2. Cerebellum and brainstem with metastatic pulmonary BSCC, coronal section. Note the focal, poorly demarcated, pale mass (*) within the white cerebellar matter. Bar, 1 cm.